Biomacromolecules

ARTICLE

pubs.acs.org/Biomac

Synthesis of Amphiphilic Tadpole-Shaped Linear-Cyclic Diblock Copolymers via Ring-Opening Polymerization Directly Initiating from Cyclic Precursors and Their Application as Drug Nanocarriers

Xuejuan Wan, Tao Liu, and Shiyong Liu*

CAS Key Laboratory of Soft Matter Chemistry, Department of Polymer Science and Engineering, Hefei National Laboratory for Physical Sciences at the Microscale, University of Science and Technology of China, Hefei, Anhui 230026, China

Supporting Information

ABSTRACT: We report on the facile synthesis of well-defined amphiphilic and thermoresponsive tadpole-shaped linear-cyclic diblock copolymers via ring-opening polymerization (ROP) directly initiating from cyclic precursors, their self-assembling behavior in aqueous solution, and the application of micellar assemblies as controlled release drug nanocarriers. Starting from a trifunctional core molecule containing alkynyl, hydroxyl, and bromine moieties, *alkynyl-(OH)-Br*, macrocyclic poly(*N*-isopropylacrylamide) (*c*-PNIPAM) bearing a single hydroxyl functionality was prepared by atom transfer radical polymerization (ATRP), the subsequent end group transformation into azide functionality, and finally the intramacromolecular ring closure reaction via click chemistry. The target amphiphilic tadpole-shaped linear-cyclic diblock copolymer, (*c*-PNIPAM)-*b*-PCL, was then synthesized via the ROP of ε-caprolactone (CL) by directly initiating from the cyclic precursor. In aqueous solution at 20 °C, (*c*-PNIPAM)-*b*-PCL self-assembles into spherical micelles consisting of hydrophobic PCL cores and well-solvated coronas of cyclic PNIPAM segments. For comparison, linear diblock copolymer with comparable molecular weight and composition, (*l*-PNIPAM)-*b*-PCL, was also synthesized. It was found that the thermoresponsive coronas of micelles self-assembled from (*c*-PNIPAM)-*b*-PCL exhibit thermoinduced collapse and aggregation at a lower critical thermal phase transition temperature (T_c) compared with those of (*l*-PNIPAM)-*b*-PCL. Temperature-dependent drug release profiles from the two types of micelles of (*c*-PNIPAM)-*b*-PCL and (*l*-PNIPAM)-*b*-PCL loaded with doxorubicin (Dox) were measured, and the underlying mechanism for the observed difference in releasing properties was proposed. Moreover, MTT assays revealed that micelles of (*c*-PNIPAM)-*b*-PCL are almost noncytotoxic up to a concentration of 1.0 g/L, whereas at the same polymer concentration, micelles loaded with Dox lead to ∼60% cell death. Overall, chain topologies of thermoresponsive block copolymers, that is, (*c*-PNIPAM)-*b*-PCL versus (*l*-PNIPAM)-*b*-PCL, play considerable effects on the self-assembling and thermal phase transition properties and their functions as controlled release drug nanocarriers.

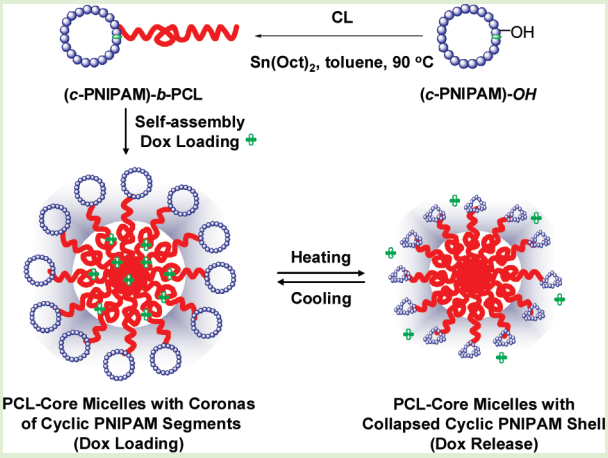

INTRODUCTION

In the past decades, enduring attention has been paid to explore the intrinsic correlation between the chain topology of block copolymers and their physical properties, self-assembling behavior in selective solvents or in bulk states, and the associated functional applications.[1−3] It has been well-established that the topological structures and chemical composition of nonlinear-shaped block copolymers can exhibit dramatic effects on the solution properties and self-assembling morphologies as compared with their linear counterpart.[4−9] It is worthy of noting that the developments of a variety of controlled radical polymerization techniques[10] such as atom transfer radical polymerization (ATRP),[11−13] reversible addition−fragmentation chain transfer (RAFT) polymerization,[14−16] and nitroxide-mediated polymerization (NMP)[17,18] have facilitated the synthesis of nonlinear-shaped polymers with varying chain architectures such as cyclic,[8,9,19−23] (miktoarm) star,[24−26] star block copolymers,[27,28] comb,[29−32] sun-shaped,[33−35] H-shaped,[36−38] and θ-shaped[39,40] polymers. Among these nonlinear chain topologies, tadpole-shaped linear-cyclic diblock copolymers[41−46] represent a special type. It is quite expected that they can self-assemble in a selective solvent into a unique type of core−shell micellar nanoparticles with the corona consisting of cyclic segments. Thus, chain entanglements within the corona region of linear-cyclic diblock micelles do not exist.

Received: December 3, 2010
Revised: January 17, 2011
Published: February 18, 2011

Furthermore, in terms of their applications, it would be quite intriguing to investigate the effects of topology and responsiveness of corona chains, that is, cyclic versus linear, on their drug release profiles if these micellar nanoparticles are to be used as triggered-release drug nanocarriers.

Considering the synthesis of tadpole-shaped linear-cyclic diblock copolymers, three typical strategies have been developed. The first one relies on the intramacromolecular ring-closure reaction under high dilution conditions, starting from specially designed linear precursor with two complementary reactive groups located at the chain middle and terminal, respectively.[43] The second one employs the intermolecular ring-closure reaction between an α,α-homobifunctional polymer precursor and a complementary bifunctional reactive reagent.[47,48] The third synthetic strategy is based on the coupling reaction between functionalized cyclic and linear polymer precursors.[45,49] Various intra- or intermolecular ring closure/coupling approaches such as electrostatic self-assembly and covalent fixation (ESA-CF),[50,51] amidation/esterification,[47,52,53] etherification reaction (hydroxyl[33] or thiol functionalities[54]), and high-efficiency and quantitative click reactions[41,42,55] have been utilized. The latter has indeed rendered the facile synthesis of macrocyclic polymers and linear-cyclic diblocks. For example, Pan et al. reported the synthesis of amphiphilic linear-cyclic diblock copolymer, (*cyclic*-polystyrene)-*b*-poly(*N*-isopropylacrylamide) ((*c*-PS)-*b*-PNIPAM), via intramacromolecular "click" ring-closure reaction of diblock precursor with two complementary reactive groups located at the chain middle and chain terminal.[41] Employing a similar approach, Li et al. synthesized amphiphilic linear-cyclic diblock copolymers consisting of PS ring and linear poly(ethylene oxide) (PEO) tail.[42] In both cases, the linear-cyclic diblocks consist of a hydrophobic macrocyclic segment and a linear hydrophilic segment. On the basis of chemical intuition, if the amphiphilic linear-cyclic diblock copolymer is composed of a linear hydrophobic and a cyclic hydrophilic block, then its micellar assemblies will consist of coronas of cyclic chain segments, which resemble those of flower-like micelles formed by ABA triblock copolymers in a selective solvent for the B block.

Previously, Winnik's and our research group have reported the synthesis of thermoresponsive macrocyclic PNIPAM via intramolecular click chemistry starting from α,ω-heterodifunctional precursors.[8,9,56] The thermoinduced aggregation behavior and the associated kinetics were also investigated.[56] We further reported the synthesis of quatrefoil-shaped star-cyclic polymers consisting of a polyhedral oligomeric silsesquioxane (POSS) core and four cyclic PS segments at the periphery,[48] and core-cross-linked micelles surface attached to macrocyclic segments.[57] Just recently, Tezuka et al.[58] and Monteiro et al.[45] independently reported the synthesis of complex-structure nonlinear polymers containing macrocyclic building motifs, such as cyclic-linear-cyclic triblock and multicyclic polymers, starting from well-defined macrocyclic precursors possessing one or two functionalities at predetermined positions. The latter two reports represent significant breakthroughs in the synthesis of nonlinear-shaped polymers containing macrocyclic elements.

On the basis of the above literature reports and our previous studies in the area of responsive polymeric assembles,[59−61] in this work, we report a novel approach for the synthesis of amphiphilic and thermoresponsive linear-cyclic diblock copolymer, (*c*-PNIPAM)-*b*-PCL, consisting of hydrophobic linear poly(ε-caprolactone) (PCL) and thermoresponsive macrocyclic PNIPAM via the ring-opening polymerization (ROP) of CL monomer directly initiating from the cyclic PNIPAM precursor bearing a single hydroxyl functionality (Scheme 1). We also investigated the self-assembly of (*c*-PNIPAM)-*b*-PCL in aqueous solution and thermal phase transition of *c*-PNIPAM corona within the micellar nanoparticles and compared with those of the linear diblock copolymer, (*l*-PNIPAM)-*b*-PCL. The temperature-dependent release profiles from drug-loaded micelles of (*c*-PNIPAM)-*b*-PCL and (*l*-PNIPAM)-*b*-PCL were also explored.

Scheme 1. Schematic Illustration for the Synthesis of Well-Defined Amphiphilic and Thermoresponsive Tadpole-Shaped Linear-Cyclic Diblock Copolymer, (*c*-PNIPAM)-*b*-PCL, and Its Self-Assembly in Aqueous Solution into Micellar Nanoparticles Consisting of PCL Cores and Coronas of Cyclic PNIPAM Segments Exhibiting Thermo-Induced Collapse and Aggregation Behavior

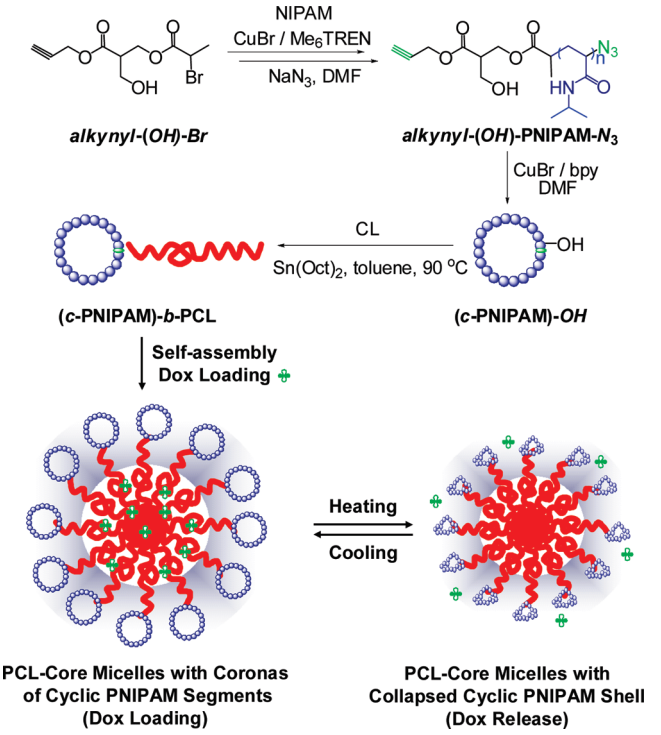

EXPERIMENTAL SECTION

Materials. *N*-Isopropylacrylamide (NIPAM, TCI) was recrystallized twice from benzene/hexane (2:1 v/v) prior to use. ε-Caprolactone (CL, Acros) was dried over CaH_2 and then distilled under vacuum just prior to use. Tris(2-aminoethyl)amine (TREN), copper(I) bromide (CuBr), 2,2-dipyridyl (bpy), stannous octoate ($Sn(Oct)_2$), Dulbecco's modified Eagle's medium (DMEM), 3-(4,5-dimethylthiazol-2-yl)-2,5-diphenyltetrazolium bromide (MTT), and doxorubicin hydrochloride (Dox·HCl) were purchased from Aldrich and used as received. The dialysis membrane (cellulose acetate) was purchased from Shanghai Green Bird Technol. Develop. with a molecular weight cutoff of 7.0 kDa. All other chemicals were purchased from Shanghai Chemical Reagent and used as received. Tris(2-(dimethylamino)ethyl)amine (Me_6TREN)[62] was synthesized according to literature procedures. The trifunctional core molecule, *alkynyl-(OH)-Br* (Scheme 1), was available from our previous study.[63]

Synthetic schemes employed for the synthesis of well-defined amphiphilic and thermoresponsive tadpole-shaped linear-cyclic diblock copolymer, (*c*-PNIPAM)-*b*-PCL, are shown in Scheme 1.

Synthesis of *alkynyl*-(*OH*)-PNIPAM-*Br*. NIPAM (4.75 g, 42 mmol), Me_6TREN (0.16 g, 0.7 mmol), *alkynyl*-(*OH*)-*Br* (0.21 g, 0.7 mmol), and 2-propanol (12 mL) were charged in a glass ampule. After the mixture was degassed via three freeze−pump−thaw cycles, CuBr (0.10 g, 0.7 mmol) was added under the protection of N_2 atmosphere. This was followed by two further freeze−pump−thaw cycles and then sealed under vacuum. The polymerization was then conducted at 30 °C for 3 h. After that, the glass ampule was soaked in liquid nitrogen to quench the polymerization. After all solvents were removed on a rotary evaporator, the residues were redissolved in CH_2Cl_2 and then passed through a neutral alumina column to remove the catalyst. The eluent was concentrated and precipitated in anhydrous diethyl ether. The sediments were collected and dried to constant weight in a vacuum oven at room temperature to yield *alkynyl*-(*OH*)-PNIPAM-*Br* as a white powder (2.86 g, 57.7% overall yield; M_n = 5500, M_w/M_n = 1.09, Figure S1 of the Supporting Information). ^{1}H NMR analysis in $CDCl_3$ revealed a degree of polymerization (DP) of 45 (Figure 2). Therefore, this polymer was denoted as *alkynyl*-(*OH*)-$PNIPAM_{45}$-*Br*.

Synthesis of *alkynyl*-(*OH*)-PNIPAM-N_3. NaN_3 (0.57 g, 8.8 mmol), *alkynyl*-(*OH*)- $PNIPAM_{45}$-*Br* (2.4 g, 0.44 mmol Br moieties), and 30 mL of DMF were charged in a 100 mL round-bottomed flask. The reaction mixture was allowed to stir at 45 °C for 48 h. After all solvents were removed at reduced pressure, the residues were dissolved in THF and passed through a neutral alumina column to remove residual sodium salts. The eluent was concentrated and then precipitated in an excess of anhydrous diethyl ether. The sediments were collected and dried to constant weight in a vacuum oven at room temperature (1.96 g, 81.7% yield; M_n = 5400, M_w/M_n = 1.08, Figure 1).

Synthesis of (*c*-PNIPAM)-*OH* by Intramolecular Click Reaction. To a 2.5 L three-necked round-bottomed flask, 1.0 L of DMF was charged and thoroughly deoxygenated by bubbling with nitrogen for 2 h. CuBr (143 mg, 1.0 mmol) and bpy (312 mg, 2.0 mmol) were introduced to the flask under the protection of N_2 flow. A separate 100 mL round-bottomed flask containing 0.2 g *alkynyl*-(*OH*)-PNIPAM-N_3 in 20 mL of DMF was degassed via two freeze/pump/thaw cycles. Under vigorous magnetic stirring and the protection of N_2, the polymer solution was slowly added to the 2.5 L flask thermostatted at 120 °C via a syringe pump at a rate of 20.0 μL/min. After the addition was completed, the reaction mixture was allowed to stir at 120 °C for another 2 h. DMF was then removed under reduced pressure, and the residues were dissolved in CH_2Cl_2 and then passed through a neutral alumina column to remove the catalyst. The eluent was concentrated under reduced pressure and then precipitated in an excess of anhydrous diethyl ether. The obtained sediments were collected and dried overnight in a vacuum oven at room temperature (117 mg, 58.5% yield; M_n = 4700, M_w/M_n = 1.08, Figure 1).

Synthesis of (*c*-PNIPAM)-*b*-PCL via Ring-Opening Polymerization Directly Initiating from (*c*-PNIPAM)-*OH*. (*c*-PNIPAM)-*OH* (0.22 g, 0.04 mmol), CL (0.37 g, 3.2 mmol), and 2.0 mL of dry toluene were added to a previously flamed glass ampule. After ~1.0 mL toluene was removed under vacuum to remove traces of water, $Sn(Oct)_2$ (0.1 mL, 0.1 mol/L in toluene) was injected in the reaction mixture. The glass ampule was carefully degassed by three freeze−pump−thaw cycles, sealed under vacuum, and placed in an oil bath thermostatted at 90 °C to start the polymerization. After 24 h, the ampule was soaked in liquid nitrogen to quench the polymerization. The reaction mixture was diluted with THF and precipitated in a large excess of petroleum ether. The sediments were collected and dried overnight in a vacuum oven at room temperature (0.39 g, 67.1% overall yield; M_n = 12 400, M_w/M_n = 1.10, Figure 1). ^{1}H NMR analysis in $CDCl_3$ revealed a DP of 60 for PCL segments (Figure 4). Therefore, this polymer was denoted as (*c*-$PNIPAM_{45}$)-*b*-PCL_{60}. For comparison, linear diblock copolymer, (*l*-PNIPAM)-*b*-PCL (M_n = 12,800, M_w/M_n = 1.12, Figure S1 of the Supporting Information), was also synthesized via ROP by using *alkynyl*-(*OH*)-$PNIPAM_{45}$-*Br* as the initiator, following similar protocols employed for the synthesis of (*l*-PNIPAM)-*b*-PCL. ^{1}H NMR analysis revealed a DP of 63 for the PCL block, and thus the linear diblock copolymer was denoted as (*l*-$PNIPAM_{45}$)-*b*-PCL_{63}.

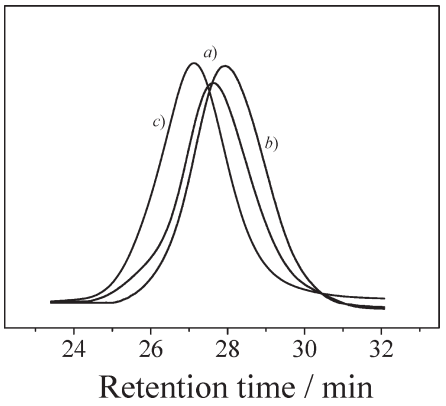

Figure 1. DMF GPC traces recorded for (a) *alkynyl*-(*OH*)-$PNIPAM_{45}$-N_3, (b) (*c*-$PNIPAM_{45}$) -*OH*, and (c) (*c*-$PNIPAM_{45}$)-*b*-PCL_{60}.

Preparation of Micellar Solutions. In a typical example, 30.0 mg (*c*-PNIPAM)-*b*-PCL was dissolved in 2 mL of DMF, and 8 mL of deionized water was added dropwise under vigorous stirring. After 12 h, DMF was removed by dialysis against deionized water using a dialysis membrane with a molecular weight cutoff of 7.0 kDa for 2 days. Stock solution with a characteristic bluish tinge was typically obtained, suggesting the formation of PCL-core micelles. The micellar solution exhibited no macroscopic phase separation upon standing at room temperature for several weeks.

Drug Loading. A mixture of Dox·HCl (20.0 mg) and 4 mL of TEA in 20 mL of DMSO was stirred overnight; then, 80.0 mg diblock copolymer was added. The solution was subjected to dialysis against PBS buffer (pH 7.4, 10.0 mM) at room temperature for 24 h, and the external buffer solution was refreshed every 6 h during this period. After this process is completed, the polymer concentration of the drug-encapsulated micellar solution was adjusted to 1.0 g/L for subsequent in vitro drug release experiments. The UV absorbance of the dialysis solution at 497 nm was recorded to determine the amount of unloaded Dox, and the encapsulation efficiency (*EE*%) was calculated as

$$EE\% = [W_{total} - W_{unloaded}] / W_{total} \times 100\%$$

The loading content (*LC*%) was calculated as

$$LC\% = [W_{loaded}] / [W_{polymer} + W_{loaded}] \times 100\%$$

where W_{total}, W_{unload}, W_{loaded}, and $W_{polymer}$ refer to the weights of drug used, unloaded drug, drug encapsulated by micelles, and diblock polymer, respectively.

In Vitro Drug Release. A 2.0 mL aqueous dispersion of drug-loaded micelles (1.0 g/L) was transferred to a dialysis tube with a molecular weight cutoff of 7.0 kDa and then immersed in 50 mL of PBS buffer solution (pH 7.4, 10 mM) thermostatted at predetermined temperatures. UV absorbance of the dialysis solution at 497 nm was monitored to determine the Dox releasing profile. A series of parallel experiments were conducted at varying buffer temperatures.

In Vitro Cytotoxicity Measurement. Cell viability was examined by the MTT assay. HeLa cells were seeded in a 96-well plate at an initial density of 5000 cells/well in 100 μL of DMEM complete medium. Free and drug-loaded micelles of (*c*-PNIPAM)-*b*-PCL were then added to achieve varying final polymer concentrations. After incubation for 4 h, MTT reagent (in 20 μL PBS buffer, 5 mg/mL) was added to each well, and the cells were further incubated with 5% CO_2 for 4 h at 37 °C. The culture medium in each well was removed and replaced by 100 μL of

DMSO. The solution from each well was transferred to another 96-well plate, and the absorbance values were recorded at a wavelength of 490 nm upon using a Thermo Electron MK3 μm. The cell viability is calculated as $A_{490,treated}/A_{490,control} \times 100\%$, where $A_{490,treated}$ and $A_{490,control}$ are the absorbance values with or without the addition of micelles, respectively. Each experiment was done in quadruple. The data were shown as the mean value plus a standard deviation ($\pm$SD).

Characterization. All ^{1}H NMR spectra were measured on a Bruker 300 MHz spectrometer using $CDCl_3$ as the solvent. Molecular weights and molecular weight distributions were determined by gel permeation chromatography (GPC) equipped with Waters1515 pump and Waters 2414 differential refractive index detector (set at 30 °C). It employs a series of three linear Styragel columns HR2, HR4, and HT5 and an oven temperature of 45 °C. The eluent was DMF at a flow rate of 1.0 mL/min. A series of low polydispersity polystyrene standards were employed for the GPC calibration. All FT-IR spectra were measured on a Bruker Vector 22 Fourier transform infrared spectrometer using the KBr disk method. The transmittance of the aqueous solutions was acquired on a Unico UV/vis 2802PCS spectrophotometer at a wavelength of 600 nm. The critical phase transition temperature, T_c, was determined by temperature-dependent turbidimetry and was defined as the temperature at which a 1% decrease in optical transmittance can be observed. Laser light scattering (LLS) measurements were operated on commercial spectrometer (ALV/DLS/SLS-5022F) equipped with a multitau digital time correlator (ALV5000) and a cylindrical 22 mW UNIPHASE He−Ne laser (λ_0 = 632 nm) as light source. Scattered light was collected at a fixed angle of 90° for duration of ~5 min. Distribution averages and particle size distributions were computed using cumulants analysis and CONTIN routines. High-resolution transmission electron microscopy (HRTEM) observation was conducted on a Hitachi H-800 electron microscope at an acceleration voltage of 200 kV. Atomic force microscope (AFM) measurement was performed on a Digital Instrument Multimode Nanoscope IIID operating in the tapping mode under ambient conditions.

RESULTS AND DISCUSSION

Synthetic approaches employed for the preparation of well-defined amphiphilic and thermoresponsive tadpole-shaped linear-cyclic diblock copolymer, (*c*-PNIPAM)-*b*-PCL, are shown in Scheme 1. We started from the trifunctional core molecule, *alkynyl*-(*OH*)-*Br*, which has been previously synthesized for the preparation of miktoarm star copolymers via the combination of ATRP, ROP, and click reaction.[63] The ATRP of NIPAM monomer by using *alkynyl*-(*OH*)-*Br* as the initiator led to *alkynyl*-(*OH*)-PNIPAM-*Br*, and this was followed by azidation into *alkynyl*-(*OH*)-PNIPAM-N_3. The subsequent intramacromolecular "click" ring closure reaction under high dilution conditions afforded macrocyclic PNIPAM bearing a single hydroxyl functionality, (*cyclic*-PNIPAM)-*OH*. Finally, the target amphiphilic and thermoresponsive linear-cyclic diblock copolymer, *c*-PNIPAM)-*b*-PCL, was synthesized via the ROP directly initiating from the cyclic precursor.

Synthesis of (*c*-PNIPAM)-*b*-PCL Diblock Copolymer. *Alkynyl*-(*OH*)-PNIPAM-*Br* precursor with a relatively narrow polydispersity was synthesized at first via the ATRP of NIPAM in 2-propanol by utilizing *alkynyl*-(*OH*)-*Br* as the initiator and CuBr/Me_6TREN as the catalyst. This polymerization system has proved to be successful and efficient for the controlled radical polymerization of NIPAM monomer, as originally reported by Stover and coworkers.[64,65] Upon reacting with an excess of NaN_3 in DMF, *alkynyl*-(*OH*)-PNIPAM-*Br* was transformed into *alkynyl*-(*OH*)-PNIPAM-N_3. ^{1}H NMR spectra of *alkynyl*-(*OH*)-PNIPAM-*Br* and *alkynyl*-(*OH*)-PNIPAM-N_3 are shown in

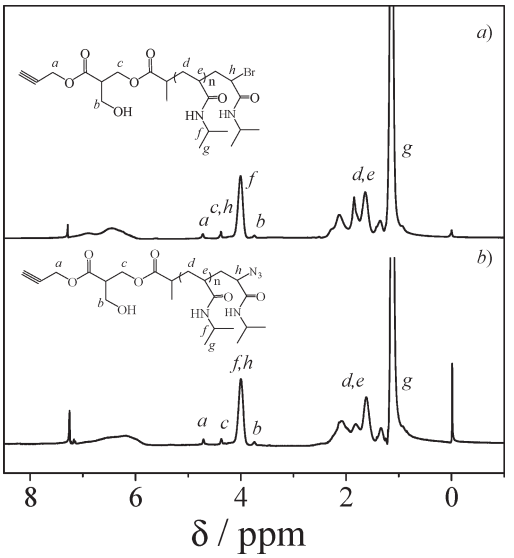

Figure 2. ^{1}H NMR spectra of (a) *alkynyl*-(*OH*)-PNIPAM$_{45}$-*Br* and (b) *alkynyl*-(*OH*)-PNIPAM$_{45}$-N_3 recorded in $CDCl_3$.

Figure 2. Resonance signals at 4.7 ppm (peak *a*) are ascribed to methylene protons of the terminal propargyl group, and signals at 3.9−4.1 ppm (peak *f*) are assigned to methenyl proton adjacent to amide residues in PNIPAM segment. On the basis of integral ratios between peaks *a* and *f*, DP of PNIPAM was calculated to be 45. Therefore, the obtained PNIPAM precursor bearing a hydroxyl and a terminal bromine moiety was denoted as *alkynyl*-(*OH*)-PNIPAM$_{45}$-*Br*. Its DMF GPC elution trace revealed a relatively narrow and symmetric peak with no tailing or shoulder at the lower or higher molecule weight side (Figure S1 of the Supporting Information), indicating the absence of premature chain termination and that *alkynyl*-(*OH*)-PNIPAM$_{45}$-*Br* can be synthesized in a controlled manner. After the terminal bromine functionality was converted to azide moiety, resonance peak *h* assigned to the methenyl proton neighboring to the azide group shifted to ~4.0 ppm. It is worthy of noting that peaks *c* and *h* in the ^{1}H NMR spectrum of *alkynyl*-(*OH*)-PNIPAM$_{45}$-*Br* overlap with each other. However, using peak *a* as a reference, we can calculate that before azidation the integral ratio of peaks *c* and *h* to peak *a* is ~1.5:1 (Figure 2a); whereas after end group transformation, the integral ratio of peaks *c* to *a* is ~1:1 (Figure 2b). This confirms the successful end group transformation from bromine to azide functionality, and the results agree quite well with those previously reported for α-*azido*-ω-*alkynyl* heterodifunctional PNIPAM.[8] DMF GPC trace of *alkynyl*-(*OH*)-PNIPAM$_{45}$-N_3 exhibits negligible changes as compared wiyh that of *alkynyl*-(*OH*)-PNIPAM$_{45}$-*Br* (Figure 1 and Figure S1 of the Supporting Information). Furthermore, a comparison of the FT-IR spectra of *alkynyl*-(*OH*)-PNIPAM$_{45}$-*Br* and *alkynyl*-(*OH*)-PNIPAM$_{45}$-N_3 in Figure 3 revealed the appearance of an absorbance peak at 2105 cm^{-1} for the latter, which is characteristic of the terminal azide moiety.

In the next step, the intramacromolecular "click" ring closure reaction of *alkynyl*-(*OH*)-PNIPAM$_{45}$-N_3 under high dilution conditions afforded the macrocyclic PNIPAM precursor bearing a single hydroxyl functionality (Scheme 1). We employed similar protocols to those previously used for the preparation of macrocylic PNIPAM from α-*azido*-ω-*alkynyl* PNIPAM.[8] Under the employed reaction conditions (120 °C, DMF, CuBr/bpy), the

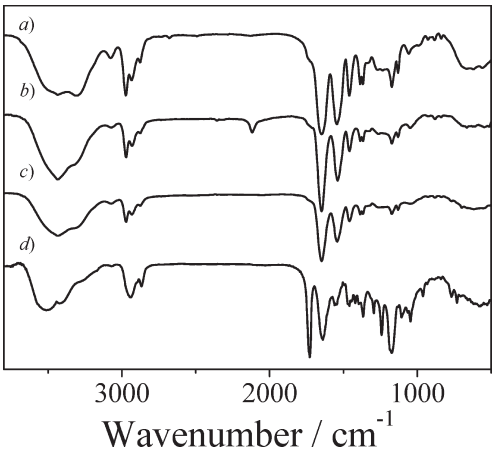

Figure 3. FT-IR spectra of (a) *alkynyl*-(*OH*)-PNIPAM$_{45}$-*Br*, (b) *alkynyl*-(*OH*)-PNIPAM$_{45}$-N_3, (c) (*c*-PNIPAM$_{45}$)-*OH*, and (d) (*c*-PNIPAM$_{45}$)-*b*-PCL$_{60}$.

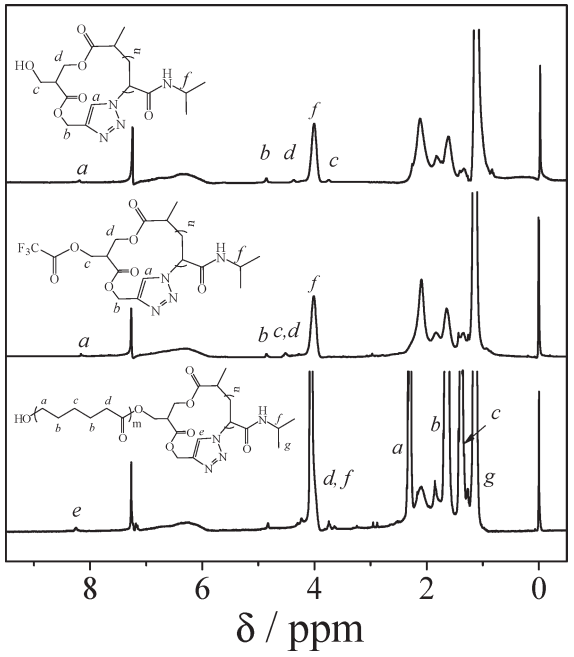

Figure 4. ^{1}H NMR spectra recorded in $CDCl_3$ for (*c*-PNIPAM$_{45}$)-*OH* (a) before and (b) after treating with trifluoroacetic anhydride, and (c) (*c*-PNIPAM$_{45}$)-*b*-PCL$_{60}$.

high efficiency of intramolecular click reaction guaranteed the fast and complete consumption of added linear precursors. ^{1}H NMR spectrum of (*c*-PNIPAM)-*OH* is shown in Figure 4a, and resonance signals ascribed to the methylene protons in propargyl moiety shifted from 4.7 ppm to 4.9 ppm (peak *b*), as compared with that of *alkynyl*-(*OH*)-PNIPAM$_{45}$-N_3. Concomitantly, a new resonance signal appeared at ~8.2 ppm, which is characteristic of the formation of 1,2,3-triazole linkages. GPC curve of (*c*-PNIPAM)-*OH* exhibited a discernible shift toward the lower molecular weight side, and the elution profile is still monomodal and symmetric, implying that the intramolecular ring closure reaction went to completion and no apparent intermolecular coupling reaction product can be discerned. This was further confirmed by the disappearance of characteristic azide (2105 cm^{-1}) absorbance peak after intramolecular click reaction, as judged from the FT-IR spectrum of (*c*-PNIPAM$_{45}$)-*OH* shown in Figure 3.

In the final step, well-defined amphiphilic tadpole-shaped linear-cyclic diblock copolymer, (*c*-PNIPAM)-*b*-PCL, was synthesized via the ROP of CL monomer at 90 °C using the cyclic precursor, (*c*-PNIPAM)-*OH*, as macroinitiator. To confirm the presence of hydroxyl functionality in the cyclic precursor, (*c*-PNIPAM)-*OH* was further treated with trifluoroacetic anhydride to form an ester linkage, and its ^{1}H NMR spectrum is shown in Figure 4b. After the esterification reaction, resonance signals ascribed to methylene protons adjacent to hydroxyl functionality (peak *c*) shifted from 3.7 to 4.5 ppm (Figure 4b). The integrated ratio of peak *c* to peak *f* (methenyl protons adjacent to amide residues of PNIPAM) is ~1:22. These results confirmed the presence of a single hydroxyl functionality in the (*c*-PNIPAM)-*OH* precursor.

The ^{1}H NMR spectrum of tadpole-shaped diblock copolymer (*c*-PNIPAM)-*b*-PCL is shown in Figure 4c. On the basis of the integral ratio of peak *a* (characteristic of PCL block) and peak *g* (characteristic of PNIPAM), the DP of PCL block was estimated to be 60, and thus the tadpole-shaped diblock copolymer was denoted as (*c*-PNIPAM$_{45}$)-*b*-PCL$_{60}$. Compared with the cyclic precursor, (*c*-PNIPAM)-*OH*, DMF GPC trace of (*c*-PNIPAM)-*b*-PCL shifted to the higher molecular weight with no tailing at the lower molecular weight side, yielding a narrow polydispersity with M_w/M_n of 1.10 (Figure 1c). This indicates that the ROP of CL monomer initiated directly from the cyclic precursor (*c*-PNIPAM)-*OH* is efficient and controllable. Moreover, FT-IR spectrum of (*c*-PNIPAM$_{45}$)-*b*-PCL$_{60}$ shown in Figure 3d clearly reveals the presence of strong absorption peak at ~1700 cm^{-1}, which is characteristic of the PCL block.

Micellization of (*c*-PNIPAM)-*b*-PCL in Aqueous Solution and Thermal Phase Transition of Micellar Coronas. Linear PNIPAM homopolymer has been well-known for its lower critical solution temperature (LCST) phase transition at ~32 °C in aqueous solution.[65] Previously, we reported that macrocyclic PNIPAM in aqueous solution possesses lower LCST, more prominent polymer concentration dependence of critical phase transition temperatures (T_c), and lower enthalpy changes (ΔH) as compared with linear PNIPAM with comparable molecular weights.[8,56] In the current study, the amphiphilic tadpole-shaped linear-cyclic diblock copolymer, (*c*-PNIPAM$_{45}$)-*b*-PCL$_{60}$, can self-assemble into micelles consisting of hydrophobic PCL cores and well-solvated *c*-PNIPAM coronas in aqueous solution at room temperature, whereas at higher temperatures, micellar coronas of cyclic PNIPAM segments will collapse and aggregate (Scheme 1). We then investigated the effects of chain topology, that is, (*c*-PNIPAM)-*b*-PCL versus (*l*-PNIPAM)-*b*-PCL, on the self-assembling behavior and the thermal phase transition of micellar coronas.

Typical hydrodynamic radius distributions, $f(R_h)$, of micellar nanoparticles self-assembled from (*c*-PNIPAM$_{45}$)-*b*-PCL$_{60}$ and (*l*-PNIPAM$_{45}$)-*b*-PCL$_{63}$ at varying temperatures are shown in Figure 5. In both cases, a bluish tinge characteristic of colloidal nanoparticles is typically observed for the micellar solutions. (*c*-PNIPAM$_{45}$)-*b*-PCL$_{60}$ micelles exhibit an average hydrodynamic radius, $<R_h>$, of ~70 nm at 20 °C and a polymer concentration of 0.1 g/L. Upon heating to 40 °C, $<R_h>$ decreases to ~56 nm with a polydispersity (μ_2/Γ^2) of 0.069, indicating the thermoinduced collapse of cyclic PNIPAM coronas at temperatures higher than the T_c. Note that at such a low concentration (0.1 g/L), we can

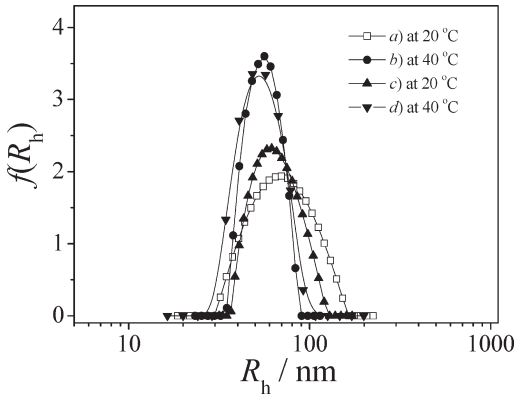

Figure 5. Typical hydrodynamic radius distributions, $f(R_h)$, obtained for micelles (0.1 g/L) of (a) (c-PNIPAM$_{45}$)-b-PCL$_{60}$ at 20 °C, (b) (c-PNIPAM$_{45}$)-b-PCL$_{60}$ at 40 °C, (c) (l-PNIPAM$_{45}$)-b-PCL$_{63}$ at 20 °C, and (d) (l-PNIPAM$_{45}$)-b-PCL$_{63}$ at 40 °C.

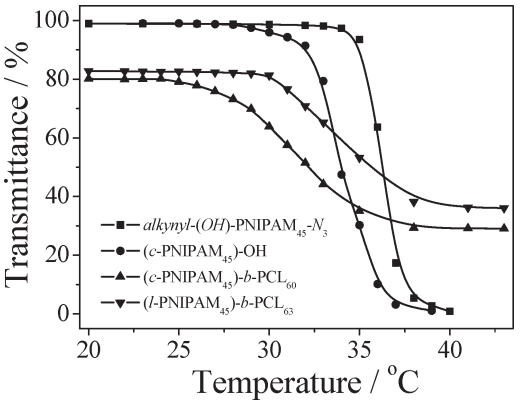

Figure 6. Temperature dependence of optical transmittance at 600 nm recorded for 2.0 g/L aqueous solutions of (a) *alkynyl*-(*OH*)-PNIPAM$_{45}$-N_3, (b) (c-PNIPAM$_{45}$)-*OH*, (c) (c-PNIPAM$_{45}$)-b-PCL$_{60}$, and (d) (l-PNIPAM$_{45}$)-b-PCL$_{63}$. The critical thermal phase transition temperature, T_c, cloud point was defined as the temperature at which a 1% decrease in optical transmittance can be observed.

only observe the collapse of micellar coronas instead of the intermicellar aggregation. This was further confirmed by the fact that scattering light intensities at a low scattering angle (15°) exhibit negligible changes for the micellar solution of (c-PNIPAM$_{45}$)-b-PCL$_{60}$ upon heating from 20 to 40 °C. Furthermore, considering the block lengths of (c-PNIPAM$_{45}$)-b-PCL$_{60}$, the micellar dimensions determined by dynamic LLS at 20 °C are much larger than the contour length of fully extended diblock copolymer chains. Therefore, to some extent, certain hydrophilic c-PNIPAM chains might be embedded within the micellar cores. This also indicates that the formed micelles are not classical spherical core−shell structured ones, and we tentatively ascribe them to large compound micelles (LCM)[66] possessing less irregular microstructures.

For the linear diblock with comparable molecular weight and composition, (l-PNIPAM$_{45}$)-b-PCL$_{63}$, its micellar assemblies exhibit $<R_h>$ values of 62 and 54 nm at 20 and 40 °C, respectively. It is interesting to note that micelles of (c-PNIPAM$_{45}$)-b-PCL$_{60}$ are larger than those of (l-PNIPAM$_{45}$)-b-PCL$_{63}$. This implies that macrocyclic PNIPAM segments have lower stabilization capability as compared with that of linear PNIPAM chains. This is understandable considering that cyclic chains exhibit more stringent restrictions on backbone conformations and NIPAM repeating units within cyclic PNIPAM segments possess weaker hydrogen bonding interaction with water molecules, as compared with those of linear PNIPAM segments.[56] HRTEM and AFM observations were further performed to examine the actual morphologies of micelles formed from (c-PNIPAM$_{45}$)-b-PCL$_{60}$ (Figure S2 of the Supporting Information). Both images clearly revealed the presence of spherical nanoparticles, which should consist of hydrophobic PCL cores stabilized by thermoresponsive c-PNIPAM coronas.

Figure 6 shows the temperature dependence of optical transmittance at 600 nm for *alkynyl*-(*OH*)-PNIPAM$_{45}$-N_3, (c-PNIPAM$_{45}$)-*OH*, micelles of (c-PNIPAM$_{45}$)-b-PCL$_{60}$ and (l-PNIPAM$_{45}$)-b-PCL$_{63}$ in aqueous solutions. It is worthy of noting that during temperature- dependent turbidity measurements, the polymer concentration is 2.0 g/L. For linear *alkynyl*-(*OH*)-PNIPAM$_{45}$-N_3, the optical transmittance exhibits abrupt changes above a critical phase transition temperature, T_c, of 35 °C; whereas for (c-PNIPAM$_{45}$)-*OH* in aqueous solution, T_c deceases to 29 °C. This is in good agreement with our previous results concerning the thermal phase transition of cyclic-PNIPAM and linear-PNIPAM.[8] For micellar solutions of (c-PNIPAM$_{45}$)-b-PCL$_{60}$ and (l-PNIPAM$_{45}$)-b-PCL$_{63}$, T_c values were determined to be 25 and 30 °C, respectively. The decrease in T_c for cyclic and linear PNIPAM segments within micellar coronas relative to those of free chains in aqueous solution can be ascribed to two factors. First, the high local chain density of PNIPAM chains within the micellar corona can lead to lower T_c, and the same phenomenon has been observed for PNIPAM brush grafted at the surface gold[67] and silica nanoparticles[68] and at the periphery of hyperbranched polymers.[69] Second, hydrophilic PNIPAM segments are covalently attached to the surface of hydrophobic PCL core, and this will also lead to the decrease in T_c. Previously, it has been well-established that when NIPAM was copolymerized with hydrophilic or hydrophobic monomers, its phase transition temperature will concomitantly increase or decrease.[70,71] In the current case, the decrease in T_c for thermoresponsive micellar coronas of (c-PNIPAM$_{45}$)-b-PCL$_{60}$ relative to that of c-PNIPAM$_{45}$ (∼5 °C decrease) revealed that the same principle as that for linear diblock copolymers; that is, the effects of local chain density and neighboring hydrophobic moieties on the thermal phase transitions also hold true for thermoresponsive tadpole-shaped diblock copolymer. Moreover, we can expect that cyclic PNIPAM segments within micellar coronas of (c-PNIPAM$_{45}$)-b-PCL$_{60}$ will not exhibit any chain entanglement, and this might exert considerable effects on their drug release profiles when (c-PNIPAM$_{45}$)-b-PCL$_{60}$ micelles are used as drug nanocarriers.

Drug Release Profiles and Cytotoxicity of (c-PNIPAM)-b-PCL Micellar Nanocarriers. Dox and the diblock copolymer were first dissolved in a cosolvent (DMSO), and the mixture was then subjected to dialysis against PBS buffer at room temperature. The UV absorbance of the dialysis solution at 497 nm was recorded to determine the amount of unloaded Dox against a standard calibration curve (Figure S3 of the Supporting Information), which was used to calculate the drug loading content (LC%) and the encapsulation efficiency (EE%).[72−74] The Dox-encapsulated micellar solution was then utilized for the subsequent in vitro drug release experiments. Figure 7 shows the time dependence of cumulative Dox release profiles from drug-loaded two types of micelles into buffer solutions at varying temperatures. For micelles assembled from (c-PNIPAM$_{45}$)-b-PCL$_{60}$, the

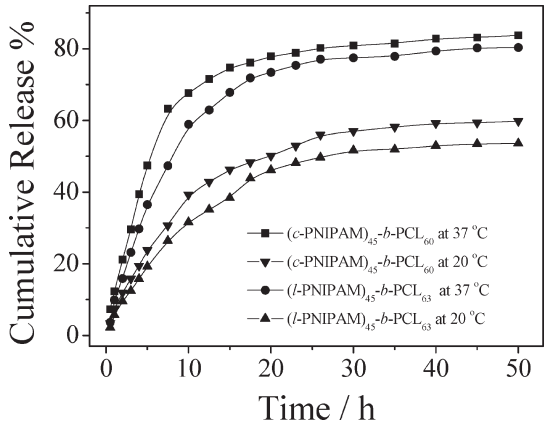

Figure 7. Cumulative Dox release from drug-loaded micelles of (a) (c-PNIPAM$_{45}$)-b-PCL$_{60}$ at 25 °C, (b) (c-PNIPAM$_{45}$)-b-PCL$_{60}$ at 37 °C, (c) (l-PNIPAM$_{45}$)-b-PCL$_{63}$ at 25 °C, and (d) (l-PNIPAM$_{45}$)-b-PCL$_{63}$ at 37 °C.

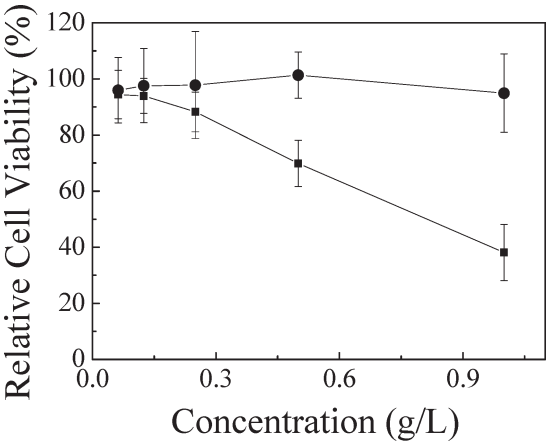

Figure 8. Relative cell viability values of HeLa cells evaluated by MTT assay after incubation with (a) micellar solution of (c-PNIPAM$_{45}$)-b-PCL$_{60}$ and (b) Dox-loaded micellar solution of (c-PNIPAM$_{45}$)-b-PCL$_{60}$ at 37 °C and varying polymer concentrations.

drug encapsulation efficiency, *EE*%, and drug loading content, *LC*%, values are 26.3 and 6.2%, respectively. As the drug-loaded micelle solution was placed in pH 7.4 buffer (PBS, 10.0 mM) at 20 °C, ∼55% of the loaded drug can be released after 50 h. When the buffer temperature increased to 37 °C, which is higher than the critical thermal phase transition temperature of the thermoresponsive micellar corona, enhanced release rate of Dox can be clearly observed, and ∼84% of the loaded drug can be released after 50 h. In both cases, most of the drug molecules are actually released within the first 20 h (∼50% at 20 °C and ∼78% at 37 °C). These results are in good agreement with those reported by Okano et al.,[75] who reported that at elevated temperatures, drug release rate from micelles of thermoresponsive amphiphilic diblock copolymer micelles can be accelerated. The collapse of thermoresponsive PNIPAM coronas at elevated temperatures leads to a much thinner micelle corona and also the partial deformation of hydrophobic cores, resulting in the faster drug release. As a comparison, we further found that for micelles of linear diblock copolymer, (l-PNIPAM$_{45}$)-b-PCL$_{63}$, the *EE*% and *LC*% values are 21.6 and 5.1%, respectively, which are slightly lower than those of (c-PNIPAM$_{45}$)-b-PCL$_{60}$. An interesting feature we can note from Figure 7 is that as compared with those of (l-PNIPAM$_{45}$)-b-PCL$_{63}$, drug-loaded micelles of (c-PNIPAM$_{45}$)-b-PCL$_{60}$ systematically exhibit higher release rate at temperatures both below and higher than the T_c, although the difference is not that significant. This should be ascribed to the presence of cyclic PNIPAM chain segments within the micellar corona of the latter, and the absence of any chain entanglements within the collapsed micellar corona can facilitate the diffusion of drug molecules out of the micelles. Besides, the collapse of thermoresponsive c-PNIPAM and l-PNIPAM segments leads to much thinner and denser micelle coronas accompanied by the deformation and reconstruction of micellar cores. In the former case, the cyclic conformation of c-PNIPAM might result in more prominent effects on the restructuring of PCL segments within micellar cores.

Finally, we examined the in vitro cell cytotoxicity of (c-PNIPAM$_{45}$)-b-PCL$_{60}$ via the MTT assay (Figure 8). HeLa cells were treated with free micelles and Dox-loaded micelles, respectively. The cell viability of micelles without drug loading could remain at ∼95% at a polymer concentration up to 1.0 g/L, clearly revealing that the micellar nanocarrier is almost noncytotoxic. When HeLa cells were incubated with Dox-loaded micelles for 4 h at pH 7.4, cell viability remained at ∼90% at low concentrations (0.05 to 0.2 g/L). As the micelle concentration increased from 0.25 to 1.0 g/L, the cell viability decreased abruptly, and only ∼38% cells survive at a final polymer concentration of 1.0 g/L, indicating that Dox-loaded micelles can enter effectively into HeLa cells and exhibit therapeutic effect to some extent.

CONCLUSIONS

In conclusion, we report a novel approach for the synthesis of amphiphilic and thermoresponsive linear-cyclic diblock copolymer, (c-PNIPAM)-b-PCL, consisting of hydrophobic linear PCL and thermoresponsive macrocyclic PNIPAM via the ROP of CL monomer directly initiating from the cyclic PNIPAM precursor bearing a single hydroxyl functionality. Compared with those of the linear diblock copolymer with comparable molecular weight and composition, (l-PNIPAM)-b-PCL, thermoresponsive micelles self-assembled from (c-PNIPAM)-b-PCL exhibit lower critical thermal phase transition temperature (T_c) and improved drug loading and releasing capacity, and the underlying mechanism for the observed difference in releasing properties was tentatively proposed. In vitro cell cytotoxicity experiments revealed that micelles of (c-PNIPAM)-b-PCL are almost noncytotoxic up to a concentration of 1.0 g/L, whereas Dox-loaded micelles cause ∼60% cell death at the same polymer concentration. These results indicate that chain topologies of thermoresponsive block copolymers, that is, (c-PNIPAM)-b-PCL versus (l-PNIPAM)-b-PCL, exert considerable effects on the self-assembling and thermal phase transition properties and their functions as controlled release drug nanocarriers.

ASSOCIATED CONTENT

Supporting Information. Analytical/spectroscopic data of GPC, TEM, AFM, and UV−vis measurements. This material is available free of charge via the Internet at http://pubs.acs.org.

AUTHOR INFORMATION

Corresponding Author
*E-mail: sliu@ustc.edu.cn.

■ ACKNOWLEDGMENT

The financial support from National Natural Scientific Foundation of China (NNSFC) project (20874092, 91027026, and 51033005), Fundamental Research Funds for the Central Universities, and Specialized Research Fund for the Doctoral Program of Higher Education (SRFDP) is gratefully acknowledged.

■ REFERENCES

(1) Hadjichristidis, N.; Pitsikalis, M.; Pispas, S.; Iatrou, H. *Chem. Rev.* **2001**, *101*, 3747–3792.
(2) Hadjichristidis, N.; Pitsikalis, M.; Iatrou, H. *Adv. Polym. Sci.* **2005**, *189*, 1–124.
(3) Inoue, K. *Adv. Polym. Sci.* **2000**, *25*, 453–571.
(4) Pispas, S.; Hadjichristidis, N.; Potemkin, I.; Khokhlov, A. *Macromolecules* **2000**, *33*, 1741–1746.
(5) Cai, Y. L.; Tang, Y. Q.; Armes, S. P. *Macromolecules* **2004**, *37*, 9728–9737.
(6) Ge, Z. S.; Zhou, Y. M.; Xu, J.; Liu, H. W.; Chen, D. Y.; Liu, S. Y. *J. Am. Chem. Soc.* **2009**, *131*, 1628–1629.
(7) Li, C. H.; Hu, J. M.; Yin, J.; Liu, S. Y. *Macromolecules* **2009**, *42*, 5007–5016.
(8) Xu, J.; Ye, J.; Liu, S. Y. *Macromolecules* **2007**, *40*, 9103–9110.
(9) Qiu, X. P.; Tanaka, F.; Winnik, F. M. *Macromolecules* **2007**, *40*, 7069–7071.
(10) Braunecker, W. A.; Matyjaszewski, K. *Prog. Polym. Sci.* **2007**, *32*, 93–146.
(11) Matyjaszewski, K.; Xia, J. H. *Chem. Rev.* **2001**, *101*, 2921–2990.
(12) Coessens, V.; Pintauer, T.; Matyjaszewski, K. *Prog. Polym. Sci.* **2001**, *26*, 337–377.
(13) Patten, T. E.; Matyjaszewski, K. *Adv. Mater.* **1998**, *10*, 901–915.
(14) Chiefari, J.; Chong, Y. K.; Ercole, F.; Krstina, J.; Jeffery, J.; Le, T. P. T.; Mayadunne, R. T. A.; Meijs, G. F.; Moad, C. L.; Moad, G.; Rizzardo, E.; Thang, S. H. *Macromolecules* **1998**, *31*, 5559–5562.
(15) Chong, Y. K.; Le, T. P. T.; Moad, G.; Rizzardo, E.; Thang, S. H. *Macromolecules* **1999**, *32*, 2071–2074.
(16) Perrier, S.; Takolpuckdee, P. *J. Polym. Sci., Part A: Polym. Chem.* **2005**, *43*, 5347–5393.
(17) Hawker, C. J.; Bosman, A. W.; Harth, E. *Chem. Rev.* **2001**, *101*, 3661–3688.
(18) Cheng, C.; Qi, K.; Khoshdel, E.; Wooley, K. L. *J. Am. Chem. Soc.* **2006**, *128*, 6808–6809.
(19) Bielawski, C. W.; Benitez, D.; Grubbs, R. H. *Science* **2002**, *297*, 2041–2044.
(20) Laurent, B. A.; Grayson, S. M. *J. Am. Chem. Soc.* **2006**, *128*, 4238–4239.
(21) Ge, Z. S.; Zhou, Y. M.; Xu, J.; Liu, H. W.; Chen, D. Y.; Liu, S. Y. *J. Am. Chem. Soc.* **2009**, *131*, 1628–1629.
(22) Kricheldorf, H. R. *J. Polym. Sci., Part A: Polym. Chem.* **2010**, *48*, 251–284.
(23) Honda, S.; Yamamoto, T.; Tezuka, Y. *J. Am. Chem. Soc.* **2010**, *132*, 10251–10253.
(24) Sun, J.; Deng, C.; Chen, X. S.; Yu, H. J.; Tian, H. Y.; Sun, J. R.; Jing, X. B. *Biomacromolecules* **2007**, *8*, 1013–1017.
(25) Karatzas, A.; Iatrou, H.; Hadjichristidis, N.; Inoue, K.; Sugiyama, K.; Hirao, A. *Biomacromolecules* **2008**, *9*, 2072–2080.
(26) Rao, J. Y.; Zhang, Y. F.; Zhang, J. Y.; Liu, S. Y. *Biomacromolecules* **2008**, *9*, 2586–2593.
(27) Hedrick, J. L.; Trollsas, M.; Hawker, C. J.; Atthoff, B.; Claesson, H.; Heise, A.; Miller, R. D.; Mecerreyes, D.; Jerome, R.; Dubois, P. *Macromolecules* **1998**, *31*, 8691–8705.
(28) Choi, Y. R.; Bae, Y. H.; Kim, S. W. *Macromolecules* **1998**, *31*, 8766–8774.
(29) Beers, K. L.; Gaynor, S. G.; Matyjaszewski, K.; Sheiko, S. S.; Moller, M. *Macromolecules* **1998**, *31*, 9413–9415.
(30) Ostmark, E.; Harrisson, S.; Wooley, K. L.; Malmstrom, E. E. *Biomacromolecules* **2007**, *8*, 1138–1148.
(31) Zhang, M. F.; Muller, A. H. E. *J. Polym. Sci., Part A: Polym. Chem.* **2005**, *43*, 3461–3481.
(32) Zhang, J. Y.; Zhou, Y. M.; Zhu, Z. Y.; Ge, Z. S.; Liu, S. Y. *Macromolecules* **2008**, *41*, 1444–1454.
(33) Pang, X. C.; Wang, G. W.; Jia, Z. F.; Liu, C.; Huang, J. L. *J. Polym. Sci., Part A: Polym. Chem.* **2007**, *45*, 5824–5837.
(34) Pang, X. C.; Jing, R. K.; Huang, J. L. *Polymer* **2008**, *49*, 893–900.
(35) Li, H. Y.; Jerome, R.; Lecomte, P. *Macromolecules* **2008**, *41*, 650–654.
(36) Iatrou, H.; Willner, L.; Hadjichristidis, N.; Halperin, A.; Richter, D. *Macromolecules* **1996**, *29*, 581–591.
(37) Li, Y. G.; Shi, P. J.; Pan, C. Y. *Macromolecules* **2004**, *37*, 5190–5195.
(38) Xu, J.; Ge, Z. S.; Zhu, Z. Y.; Luo, S. Z.; Liu, H. W.; Liu, S. Y. *Macromolecules* **2006**, *39*, 8178–8185.
(39) Shi, G. Y.; Pan, C. Y. *J. Polym. Sci., Part A: Polym. Chem.* **2009**, *47*, 2620–2630.
(40) Tezuka, Y.; Tsuchitani, A.; Yoshioka, Y.; Oike, H. *Macromolecules* **2003**, *36*, 65–70.
(41) Shi, G. Y.; Tang, X. Z.; Pan, C. Y. *J. Polym. Sci., Part A: Polym. Chem.* **2008**, *46*, 2390–2401.
(42) Dong, Y. Q.; Tong, Y. Y.; Dong, B. T.; Du, F. S.; Li, Z. C. *Macromolecules* **2009**, *42*, 2940–2948.
(43) Beinat, S.; Schappacher, M.; Deffieux, A. *Macromolecules* **1996**, *29*, 6737–6743.
(44) Li, L. Y.; He, W. D.; Li, J.; Han, S. C.; Sun, X. L.; Zhang, B. Y. *J. Polym. Sci., Part A: Polym. Chem.* **2009**, *47*, 7066–7077.
(45) Monteiro, M. J.; Lonsdale, D. E. *Chem. Commun.* **2010**, *46*, 7945–7947.
(46) Li, H. Y.; Riva, R.; Jerome, R.; Lecomte, P. *Macromolecules* **2007**, *40*, 824–831.
(47) Kubo, M.; Hayashi, T.; Kobayashi, H.; Itoh, T. *Macromolecules* **1998**, *31*, 1053–1057.
(48) Ge, Z. S.; Wang, D.; Zhou, Y. M.; Liu, H. W.; Liu, S. Y. *Macromolecules* **2009**, *42*, 2903–2910.
(49) Adachi, K.; Irie, H.; Sato, T.; Uchibori, A.; Shiozawa, M.; Tezuka, Y. *Macromolecules* **2005**, *38*, 10210–10219.
(50) Tezuka, Y.; Oike, H. *J. Am. Chem. Soc.* **2001**, *123*, 11570–11576.
(51) Oike, H.; Uchibori, A.; Tsuchitani, A.; Kim, H. K.; Tezuka, Y. *Macromolecules* **2004**, *37*, 7595–7601.
(52) Kubo, M.; Hayashi, T.; Kobayashi, H.; Tsuboi, K.; Itoh, T. *Macromolecules* **1997**, *30*, 2805–2807.
(53) Lepoittevin, B.; Perrot, X.; Masure, M.; Hemery, P. *Macromolecules* **2001**, *34*, 425–429.
(54) Whittaker, M. R.; Goh, Y. K.; Gemici, H.; Legge, T. M.; Perrier, S.; Monteiro, M. J. *Macromolecules* **2006**, *39*, 9028–9034.
(55) Han, D. H.; Tong, X.; Zhao, Y.; Galstian, T.; Zhao, Y. *Macromolecules* **2010**, *43*, 3664–3671.
(56) Ye, J.; Xu, J.; Hu, J. M.; Wang, X. F.; Zhang, G. Z.; Liu, S. Y.; Wu, C. *Macromolecules* **2008**, *41*, 4416–4422.
(57) Peng, Y.; Liu, H. W.; Zhang, X. Y.; Liu, S. Y.; Li, Y. S. *Macromolecules* **2009**, *42*, 6457–6462.
(58) Sugai, N.; Heguri, H.; Ohta, K.; Meng, Q. Y.; Yamamoto, T.; Tezuka, Y. *J. Am. Chem. Soc.* **2010**, *132*, 14790–14802.
(59) Ge, Z. S.; Liu, S. Y. *Macromol. Rapid Commun.* **2009**, *30*, 1523–1532.
(60) Hu, J. M.; Liu, S. Y. *Macromolecules* **2010**, *43*, 8315–8330.
(61) Xu, J.; Liu, S. Y. *Soft Matter* **2008**, *4*, 1745–1749.
(62) Clampolini, M.; Nardi, N. *Inorg. Chem.* **1966**, *5*, 41–44.
(63) Zhang, Y. F.; Li, C. H.; Liu, S. Y. *J. Polym. Sci., Part A: Polym. Chem.* **2009**, *47*, 3066–3077.
(64) Xia, Y.; Yin, X. C.; Burke, N. A. D.; Stover, H. D. H. *Macromolecules* **2005**, *38*, 5937–5943.
(65) Xia, Y.; Burke, N. A. D.; Stover, H. D. H. *Macromolecules* **2006**, *39*, 2275–2283.
(66) Cameron, N. S.; Corbierre, M. K.; Eisenberg, A. *Can. J. Chem.* **1999**, *77*, 1311–1326.

(67) Zhu, M. Q.; Wang, L. Q.; Exarhos, G. J.; Li, A. D. Q. *J. Am. Chem. Soc.* **2004**, *126*, 2656–2657.
(68) Wu, T.; Zhang, Y. F.; Wang, X. F.; Liu, S. Y. *Chem. Mater.* **2008**, *20*, 101–109.
(69) Luo, S. Z.; Xu, J.; Zhu, Z. Y.; Wu, C.; Liu, S. Y. *J. Phys. Chem. B* **2006**, *110*, 9132–9139.
(70) Liu, B.; Perrier, S. *J. Polym. Sci., Part A: Polym. Chem.* **2005**, *43*, 3643–3654.
(71) Alarcon, C. D. H.; Pennadam, S.; Alexander, C. *Chem. Soc. Rev.* **2005**, *34*, 276–285.
(72) Oh, J. K.; Siegwart, D. J.; Lee, H. I.; Sherwood, G.; Peteanu, L.; Hollinger, J. O.; Kataoka, K.; Matyjaszewski, K. *J. Am. Chem. Soc.* **2007**, *129*, 5939–5945.
(73) Sun, H. L.; Guo, B. N.; Li, X. Q.; Cheng, R.; Meng, F. H.; Liu, H. Y.; Zhong, Z. Y. *Biomacromolecules* **2010**, *11*, 848–854.
(74) Zhang, W. L.; Li, Y. L.; Liu, L. X.; Sun, Q. Q.; Shuai, X. T.; Zhu, W.; Chen, Y. M. *Biomacromolecules* **2010**, *11*, 1331–1338.
(75) Chung, J. E.; Yokoyama, M.; Yamato, M.; Aoyagi, T.; Sakurai, Y.; Okano, T. *J. Controlled Release* **1999**, *62*, 115–127.